In vivo validation of a miniaturized electrochemical oxygen sensor for measuring intestinal oxygen tension

Original Research Article

Full Title: ***In Vivo*** **Validation of a Miniaturised Electrochemical Oxygen Sensor for Measuring Intestinal Oxygen Tension**

Running Title: Miniaturised Sensor for Measuring Intestinal ptO_2

Article type: Original research article; not based on any previous communications to a society or meeting

Mark E Gray [a,b,*], Jamie R K Marland [c], Camelia Dunare [c], Ewen O Blair [c], James Meehan [b], Andreas Tsiamis [c], Ian H Kunkler [b], Alan F Murray [c], David Argyle [a], Alex Dyson [d], Mervyn Singer [d], Mark A Potter [e]

[a] *The Royal (Dick) School of Veterinary Studies and Roslin Institute, University of Edinburgh, Easter Bush, Roslin, Midlothian, Edinburgh, EH25 9RG, United Kingdom*.
[b] *Cancer Research UK Edinburgh Centre and Division of Pathology Laboratories, Institute of Genetics and Molecular Medicine, University of Edinburgh, Crewe Road South, Edinburgh, EH4 2XU, United Kingdom*.
[c] *School of Engineering, Institute for Integrated Micro and Nano Systems, The King's Buildings, Edinburgh, EH9 3FF, United Kingdom*.
[d] *Bloomsbury Institute of Intensive Care Medicine, Division of Medicine, University College London, Gower Street, London, WC1E 6BT, United Kingdom.*
[e] *Department of Surgery, Western General Hospital, Crewe Road, Edinburgh, EH4 2XU, United Kingdom.*

*__Corresponding author:__ **Mark E Gray**.
Address: The Royal (Dick) School of Veterinary Studies and Roslin Institute, University of Edinburgh, Easter Bush, Roslin, Midlothian, Edinburgh, EH25 9RG, United Kingdom.
Telephone: +44 (0)131 5371763. **E-mail address:** s9900757@sms.ed.ac.uk

Acknowledgment and funding source: This work was supported by funding from the UK Engineering and Physical Sciences Research Council, through the IMPACT programme grant (EP/K-34510/1) and a project grant from Bowel and Cancer Research UK.

Abstract

Recent advances in the fields of electronics and microfabrication techniques have led to the development of implantable medical devices for use within the field of precision medicine. Monitoring visceral surface tissue O_2 tension (ptO_2) by means of an implantable sensor is potentially useful in many clinical situations, including the peri-operative management of patients undergoing intestinal resection and anastomosis. This concept could provide a means by which treatment could be tailored to individual patients. This study describes the *in vivo* validation of a novel miniaturised electrochemical O_2 sensor to provide real-time data on intestinal ptO_2. A single O_2 sensor was placed onto the serosal surface of the small intestine of anaesthetised rats that were exposed to ischaemic (superior mesenteric artery occlusion) and hypoxaemic (alterations in inspired fractional O_2 concentrations) insults. Control experiments demonstrated that the sensors function and remain stable in an *in vivo* environment. Intestinal ptO_2 decreased following superior mesenteric artery occlusion and with reductions in inspired O_2 concentrations. These results were reversible after reinstating blood flow or increasing inspired O_2 concentrations. We have successfully developed an anaesthetised rat intestinal ischaemic and hypoxic model for validation of a miniaturised O_2 sensor to provide real-time measurement of intestinal ptO_2. Our results support further validation of the sensors in physiological conditions using a large animal model to provide evidence of their use in clinical applications where monitoring visceral surface tissue O_2 tension is important.

Introduction

Precision medicine is beginning to play important roles in the prevention, investigation and treatment of a range of diseases as it enables individual patient variability to be considered. Precision medicine may be integrated into standard clinical practices in different ways, however, recent advances in the fields of electronics and microfabrication techniques have led to interest in the use of implantable medical devices for disease diagnosis, treatment and monitoring. Pre-clinical research using *in vivo* murine studies have already shown that implantable devices can detect tumour secreted biomarkers (8) or release chemotherapeutic drugs directly within tumours (29). The biocompatibility and biofunctionality of implantable devices in a range of diseases has also been shown in many studies using *in vivo* models, providing substantial evidence of their increasing potential for clinical applications (15).

One such implantable medical device is being developed through the Implantable Microsystems for Personalised Anti-Cancer Therapy (IMPACT) programme at the University of Edinburgh (27). This project has developed a novel miniaturised implantable O_2 sensor on a silicon chip designed to monitor intra-tumoural O_2 levels. The design is based on a Clark electrode for the electrochemical detection of O_2 which is connected by a lead to external instrumentation. Hypoxic tumour areas are more resistant to radio and chemotherapy, therefore identifying them by means of an implantable sensor may enable these regions to be targeted more efficiently. However, the use of this sensor may not be restricted to cancer patients and may have additional applications in which monitoring visceral surface tissue O_2 tension (ptO_2) is clinically important. One potential situation where assessment of tissue perfusion would be advantageous is in the peri-operative management of patients undergoing intestinal surgery.

Intestinal resection and anastomosis is a commonly performed abdominal operation for a variety of benign and malignant diseases. The procedure involves removal (resection) of a segment of intestine with the subsequent re-joining (anastomosis) of the intestinal ends in a manner that optimises healing and restores mural and luminal integrity. However, if the anastomosis fails to heal and a leak develops, patients suffer a significant increase in morbidity (17, 23, 28) and mortality (9). Leak rates can be as high as 24% for surgery performed in the distal rectum; however, overall leak incidence is generally accepted to be approximately 6-7% (6, 21). The aetiology of an anastomotic leak is multifactorial; however, blood flow disruption, leading to compromised tissue perfusion and decreased oxygenation is known to affect anastomotic healing through the development of peri-anastomotic necrosis (38). Surgeons typically asses intra-operative intestinal perfusion through macroscopic tissue appraisal; however, this subjective technique is unable to predict the risk of a leak occurring. It is suggested that objective measurements of tissue perfusion at the anastomosis can aid the identification of anastomotic sites at increased risk of leakage (24). Methods used to assess tissue perfusion (visible light and near infrared spectroscopy and laser fluorescence angiography) (13, 19) and oxygen tensions (scanning laser Doppler flowmetry and wireless hand held pulse oximeters) (7, 38) have been shown to help predict the occurrence of a leak. Visible light spectroscopy has also been shown to be compatible with endoscopic procedures (5, 13, 25). Currently there is one clinical trial underway assessing whether the intra-operative measurement of anastomotic perfusion using a fluorescent dye (indocyanine green) and near-infrared laparoscopy can minimise the occurrence of leaks compared with conventional white-light laparoscopy (3). Pre-clinical (26, 39) and clinical (40, 41) studies have also shown that Clark O_2 sensors can not only measure intestinal ptO_2, but also predict the occurrence of an anastomotic leak. These studies used O_2 sensors consisting of a platinum cathode and

sliver anode, which were used to measure intra-operative intestinal ptO_2. Intra-operative measurements were only possible due to the large size of the electrodes used in the pre-clinical studies (62x7mm, intestinal contact surface 2mm) (39) and because hand held devices were used in both clinical studies.

Unfortunately, none of these techniques are routinely used by clinicians and are only applicable to intra-operative use; they cannot be left *in situ* as a means of real-time, continuous, post-operative monitoring. The development of a miniaturised implantable device for the continuous intra- and post-operative monitoring of intestinal ptO_2 could provide an additional means by which anastomotic healing could be monitored, thereby providing a means by which peri-operative patient treatment could optimised. In this study we describe the development and use of an anaesthetised rat intestinal ischaemic and hypoxic model for validation of the IMPACT O_2 sensor to provide real-time measurement of intestinal ptO_2.

Materials and Methods

Studies were undertaken under a UK Home Office Project Licence in accordance with the Animals (Scientific Procedures) Act 1986 and with approval from the University College London Animal Ethics Committee. Male Wistar rats (Charles River Laboratories, Margate, UK) of approximately 400 g body weight were used in all experiments (n>4/treatment group). Prior to instrumentation, the rats were acclimatised for at least 1 week and housed in cages of 4 on an alternating 12 h light/dark cycle with *ad libitum* access to food and water.

Rats were anaesthetised using isoflurane (Abbott, Maidenhead, UK) delivered in room air (5% for induction, 2% for surgical procedures and 1.5% for maintenance). Rats were placed on a heated mat to maintain rectal temperature between 36.5–37.5^{o}C, which was continuously

monitored using a temperature sensor (Harvard Apparatus, Cambridge, UK) inserted into the rectum. Placement of arterial and venous lines was performed as reported previously (10) (Fig.1). The arterial line was subsequently connected to a pressure transducer system (Powerlab and Chart 5 acquisition software, AD Instruments, Chalgrove, UK) for continuous monitoring and recording of mean arterial blood pressure and heart rate. The arterial line was also used for intermittent blood sampling; when required, 0.1 ml of arterial blood was taken into heparinised capillary tubes for blood-gas analysis (ABL90 Analyser; Radiometer, Copenhagen, Denmark). The venous line was used for administration of fluids; all animals received a continuous infusion of 10–20 ml/kg/hr compound sodium lactate (Baxter, Thetford, UK) to maintain mean arterial blood pressure at approximately 100 mmHg. A tracheostomy was created using 2.08 mm external diameter polythene tubing (Portex Ltd, Hythe, UK); this was attached to a T-piece to secure the airway, maintain anaesthesia and to allow alterations in the inspired fractional O_2 concentration (FiO_2).

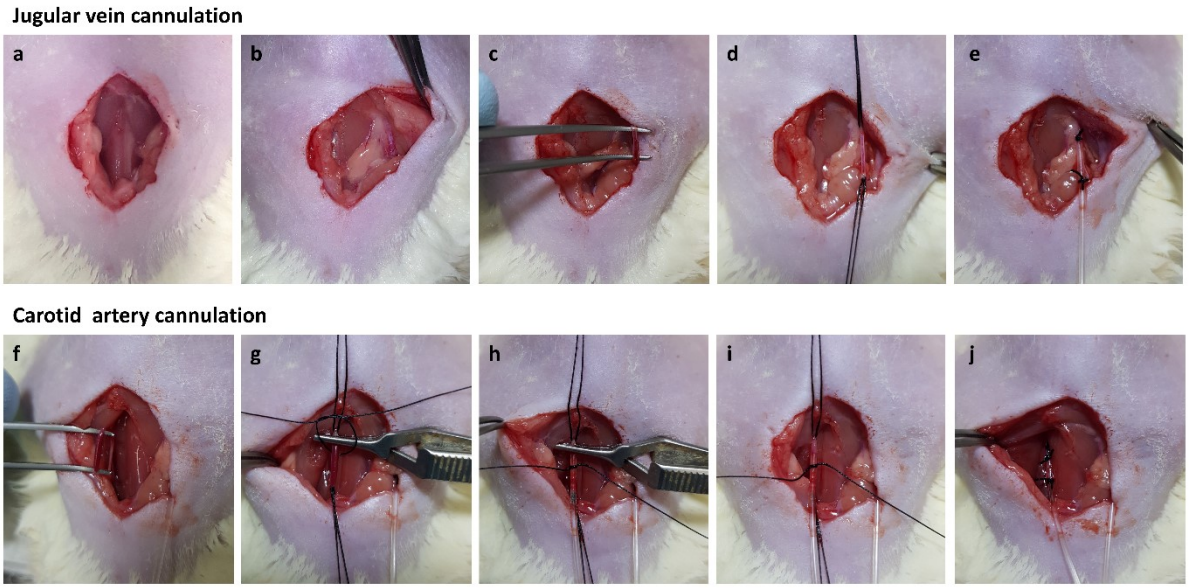

Figure 1. Intra-operative photographs depicting placement of central venous (jugular) and arterial (carotid) lines. a) A 2 cm ventral cervical skin incision is made. **b&c)** Cervical dissection is performed for identification and mobilisation of the right jugular vein. **d)** One untied suture is placed distally around the jugular vein and a second is placed proximally and tied securely, leaving approximately 1 cm of vein between the 2 sutures. **e)** A venotomy is created just distal

to the proximal suture; the cannula is inserted and advanced into the vein approximately 2-3 cm before tying the distal suture around the vein and cannula. **f)** Cervical dissection is performed for identification of the left carotid artery and its isolation from the vagus nerve. **g)** One untied suture is placed distally around the carotid artery and a second is placed proximally and tied securely leaving approximately 1.5 cm of artery between the 2 sutures. A small clamp is added just proximal to the distal suture before placing a third untied suture. **h)** An arteriotomy is created between the 2 sutures and the cannula is inserted and advanced up to the clamp. **i)** The third suture is tied loosely over the cannula and the clamp is removed. **j)** The cannula is advanced a further 2 cm before tying the distal suture around the artery and cannula. Both vessels were cannulated using 0.96 mm outside diameter PVC tubing (Scientific Commodities Inc., Lake Havasu City, AZ, USA) and secured in place with 5-0 silk (Ethicon, UK).

One control group (to assess sensor longevity and baseline drift) and two treatment groups (either superior mesenteric artery occlusion, or manipulation of FiO_2 and circulating blood volume) were used to assess whether the sensor could detect changes in intestinal oxygenation following local or systemic cardiorespiratory insults (Fig. 2). A ventral midline celiotomy was performed on all animals extending from the pubis to the manubrium and a temporary cystotomy was created by making a small stab incision at the apex of the bladder, which was then cannulated with 1.57 mm external diameter polythene tubing (Portex Ltd, Hythe, UK) and sutured in place. To allow access to the abdominal vasculature and placement of the sensor, the caecum and small intestine were exteriorised to the left side on the animal, wrapped in cling film (to reduce evaporative fluid and convective heat loss) and kept moist with regular topical applications of saline. The O_2 sensor was placed on the antimesenteric serosal surface of a proximal section of small intestine. The active area of the sensor was kept moist and placed at the midpoint between small serosal blood vessels (Fig. 3). The sensor lead was temporarily attached to the serosal surface of the bowel using tissue adhesive (Vetbond, 3M, Bracknell, UK). Following instrumentation, all animals were allowed a period of stabilisation of at least 30 min to achieve stable baseline physiological variables. Continuous sensor readings were made throughout each experiment, commencing after the initial stabilisation period and continuing for 15 min following confirmation of death post-

euthanasia. All animals were euthanised with intravenous sodium pentobarbitone (Pentoject; Animalcare, York, UK).

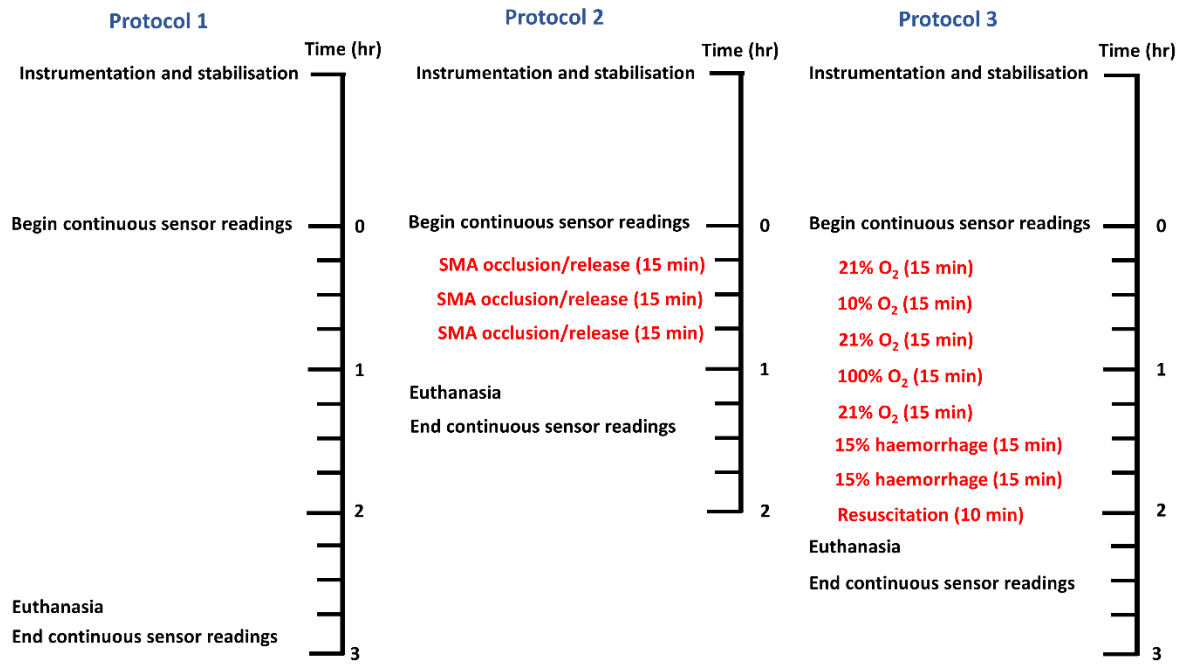

Figure 2. Outline of experimental protocols and interventions. Protocol 1: Control animals with no interventions. Protocol 2: Superior mesenteric artery occlusion. Protocol 3: Alterations in FiO_2, haemorrhage and autotransfusion (resuscitation). Instrumentation encompassed: anaesthesia induction, surgical preparation, placement of arterial and venous lines and celiotomy. The sensor was placed on the serosal surface of the small intestine approximately half way through the stabilisation period. Continuous sensor readings were commenced following the achievement of stable baseline physiological variables and continued for 15 min following confirmation of death post-euthanasia.

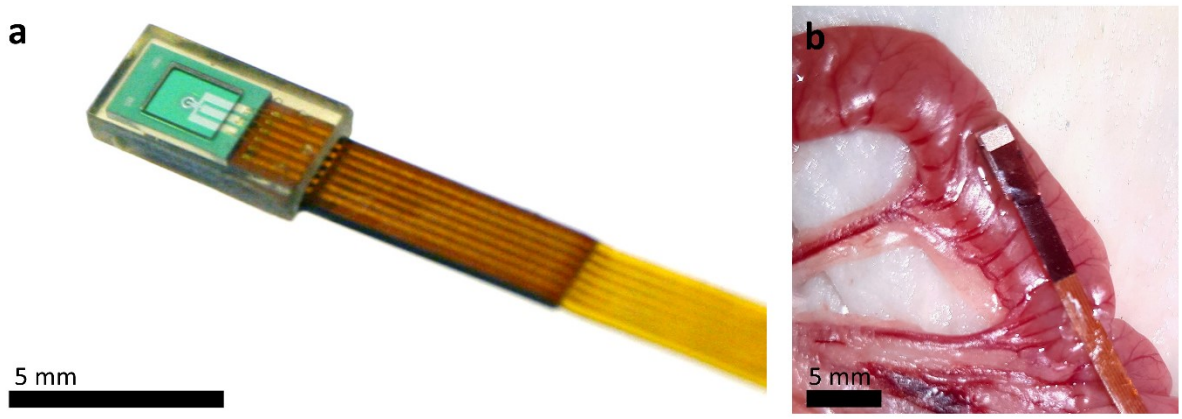

Figure 3. Sensor picture and intra-operative photographs depicting intestinal placement of the sensor. a) Macroscopic image of the IMPACT miniaturised O_2 sensor. **b)** Intra-operative sensor placement on the serosal surface of a section of small intestine.

Oxygen Sensor Recordings

The IMPACT O_2 sensor contains a complete miniaturised three-electrode cell, with platinum working and counter electrodes, and a silver/silver chloride reference electrode. Nafion was used to cover the electrode surfaces to reduce electrode biofouling and improve sensor lifetime. Electrodes were fabricated on silicon wafers using conventional microfabrication techniques, and diced into 2.0 mm x 3.0 mm chips, each of which carried a single sensor (Marland *et al*., manuscript submitted). Chips were wire bonded to a 1.7 mm x 200 mm long lead, and the chip was sealed in biocompatible epoxy resin giving an overall sensor size of approximately 2.8 mm x 5.0 mm x 1.4 mm (width x length x height), with a clear window over the central active area to permit sensor access to the tissue environment. Following intestinal placement/implantation, the sensor lead was connected to an EmStat3 Blue potentiostat (PalmSens BV, Houten, Netherlands). Periodic O_2 measurements were performed using chronoamperometry at -0.5 V (versus the on-chip Ag/AgCl reference electrode) for 20 s, followed by a rest period of 20 s, repeated continuously for the duration of the experiment. The working electrode current over the final 5 s of each chronoamperometry recording was averaged using MATLAB R2017a (MathWorks, Natick, MA, USA) to derive the mean current. We have previously shown that the measured current magnitude is proportional to local pO_2 at the sensor surface in saline (Marland *et al*., manuscript submitted). However, since there may be small environmental differences between saline and tissue that could affect the slope of the sensor response *in vivo*, we chose to directly quantify its electrode current in this study.

Protocol 1: Control group

The control group of animals consisted only of continuous sensor readings taken for 165 min. These animals were sham operated, receiving only a ventral midline celiotomy (as described

in the previous section) for sensor placement with no superior mesenteric artery (SMA) occlusions or manipulations of FiO_2 or circulating blood volume being performed (i.e.no physiological challenges were performed on these instrumented animals). Arterial blood samples were obtained immediately prior to the start of continuous sensor readings, every hour thereafter and then just prior to euthanasia.

Protocol 2: Intestinal tissue responses to temporary superior mesenteric artery occlusion

For temporary SMA occlusion, the vessel was first identified originating from the left side of the aorta at the level of the right renal vein joining the caudal vena cava. The SMA was dissected free from surrounding soft tissue and its associated vein as close to its aortic origin as possible. A loose suture of 5-0 silk (Ethicon, UK) was placed round the artery for ease of location and to allow gentle traction to aid its temporary and reversible mechanical occlusion. Following its isolation, the vessel was repeatedly occluded with the use of a haemostatic clamp (Fine Science Tools, Linton, UK). Each occlusion was performed for 5 min with a 10 min reperfusion period between occlusions. Vessel occlusion was confirmed by loss of pulsations in the mesenteric arteries and intestinal pallor. A hyperaemic flush and the presence of mesenteric arterial pulsations were evident following removal of the haemostatic clamp. Arterial blood samples were obtained immediately prior to the start of continuous sensor readings and just before euthanasia.

Protocol 3: Intestinal tissue responses to alterations in inspired oxygen concentrations, progressive haemorrhage and autotransfusion

FiO_2 (1.0, 0.21, 0.1) was varied at 15 min intervals and delivered through a flowmeter via the isoflurane vaporiser to maintain adequate anaesthesia. The protocol for varying FiO_2 was: 0.21 for 15 min, 0.1 for 15 min (inducing hypoxaemia), 0.21 for 15 min, 1.0 for 15 min

(inducing hyperoxaemia) before returning to 0.21 for 15 min. Arterial blood samples were taken at the end of each FiO_2 alteration.

Following completion of the FiO_2 modifications, progressive haemorrhage was achieved by withdrawing 15% of the animals circulating blood volume (estimated based on 70 ml/kg body weight) over 5 min. The animal was allowed to stabilise for 10 min before a further 15% circulating blood volume was removed. The exsanguinated blood was collected in a heparinised syringe and maintained at 37^{o}C. Autotransfusion was performed by administering the exsanguinated blood intravenously to the animal over 10 min. Arterial blood samples were taken at the end of each haemorrhage procedure and just before euthanasia.

Statistical Analysis

Data was confirmed as normally distributed using the Shapiro-Wilk test and subsequently analysed with parametric tests; one-way ANOVA with Holm-Šídák multiple comparisons test was used to test for differences between groups; *P* values <0.05 were deemed statistically significant. Data were expressed as mean ± standard error of the mean (SEM). Statistical analyses were performed using Prism 7 (GraphPad Software, San Diego, CA, USA).

Results

Sensor readings remained stable in control animals

For assessment of sensor stability, we performed continuous sensor readings in instrumented rats which were not subjected to any physiological interventions (n=3). These control experiments were of a duration that encompassed the longest experimental protocol. The negative currents generated in the O_2 sensors are proportional to ptO_2, with more negative values indicating greater O_2 partial pressures. The measured currents were stable over 165

min, with mean values ranging from -1.14 ± 0.03 nA at 15 min to -1.44 ± 0.15 nA at 135 min (p=0.7244) (Fig. 4a).

To assess the stability of the rats during anaesthesia, physiological data including core temperature (CT), heart rate (HR), respiratory rate (RR) and mean arterial blood pressure (MAP) plus intermittent blood-gas and biochemistry samples were evaluated. All physiological data, blood-gas analysis and electrolytes remained stable; only blood glucose levels decreased slightly towards the end of the procedure. Although this reduction was not statistically significant (p= 0.9304) it is consistent with the fasting state and metabolic demands of the rat during anaesthesia (Fig 4b). The physiological data obtained, combined with arterial blood analysis, provided evidence that the rats were able to cope with the physiological demands from general anaesthesia for the duration of our experimental protocols. These results are in accordance with other previous studies (11).

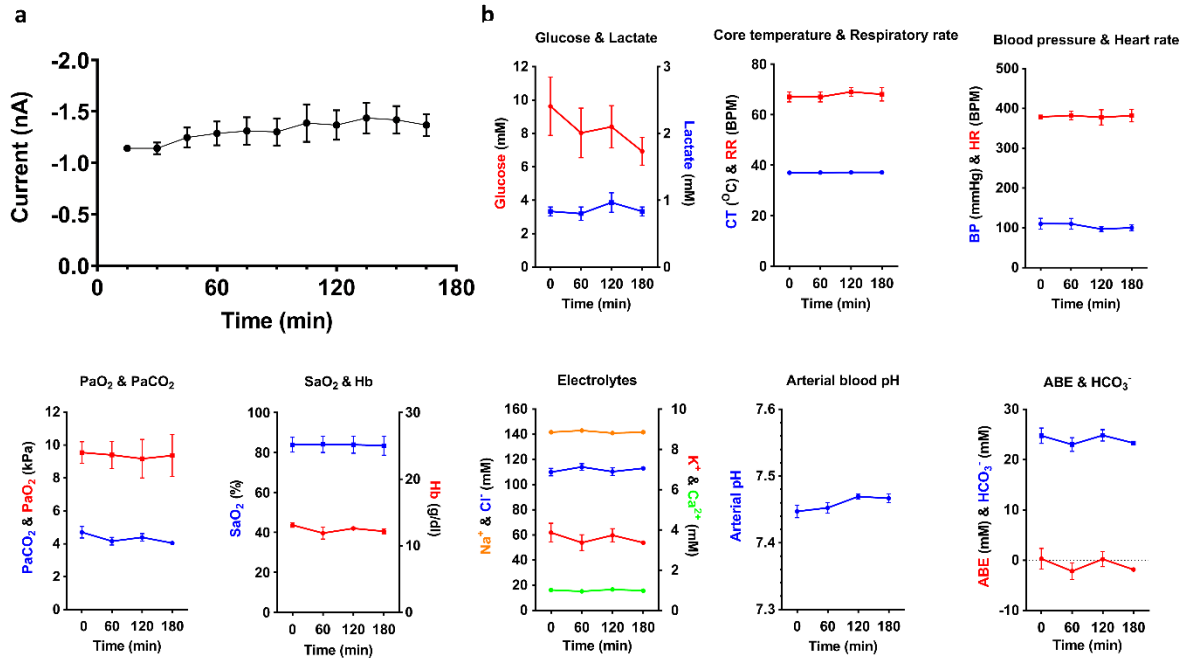

Figure 4. Sensor readings and physiological data obtained from control animals (Protocol 1). a) Current generated at the working electrode of the sensor during continuous sensor readings over a period of 165 min; results show mean current readings from the final 5 min of each 15 min period (one-way ANOVA with Holm-Šídák multiple comparisons test; data expressed as mean ± SEM, n=3, p=0.7244). **b)** Physiological data obtained throughout the

experimental period (Hb: haemoglobin; ABE: arterial base excess; SaO_2: haemoglobin O_2 saturation; PaO_2: arterial O_2 partial pressure; $PaCO_2$: arterial CO_2 partial pressure; CT: core temperature; RR: respiratory rate; HR: heart rate).

Oxygen current generated by the sensor rapidly decreased following occlusion of the superior mesenteric artery and was reversible upon reinstatement of blood flow

To assess whether the sensor could detect changes in intestinal oxygenation through the generation of localised tissue ischaemia, we performed three cycles of temporary SMA occlusion followed by release in each rat (n=4) (Fig. 5a). After each occlusion, there was an almost immediate fall in sensor current from non-occluded readings of -1.85 ± 0.05 nA to occluded readings of -0.27 ± 0.08 nA. The decrease in current that occurred during each occlusion was statistically significant when compared to current values pre- and post-occlusion (p= 0.0082). The decrease in current during the occlusion quickly rose back to non-occluded current levels following reinstatement of blood flow (Fig. 5b and Table I). Following euthanasia, sensor readings fell to the lowest recorded, measuring 0.04 ± 0.16 nA; this decrease was statistically significant when compared to non-occluded SMA currents (p= 0.0025) (Fig. 5c). These results showed that the sensor could quickly, reliably and reproducibly detect transient intestinal ischaemia.

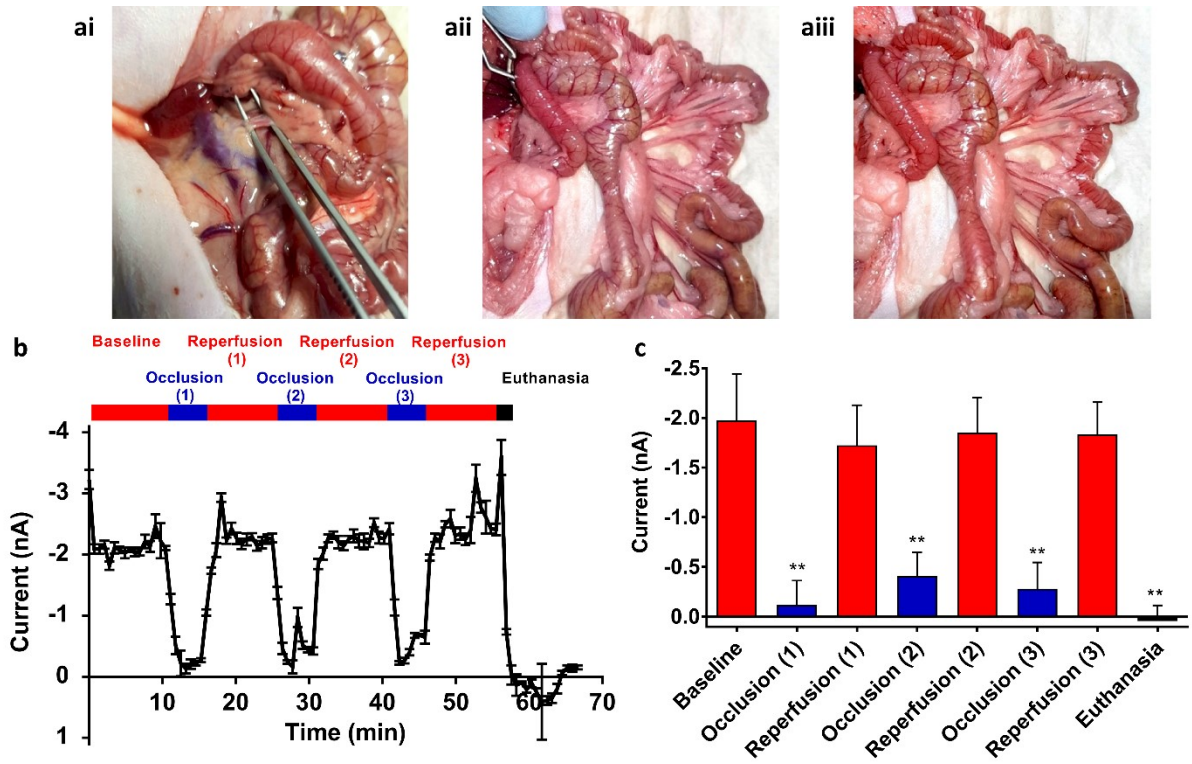

Figure 5. Intra-operative photographs and sensor readings during temporary superior mesenteric artery occlusion (Protocol 2). ai) Identification of the SMA originating from the left side of the aorta at the level of the right renal vein joining the caudal vena cava; the vessel is robust and can withstand the manipulation required for isolation from its surrounding tissue and associated vein. **aii)** A Bulldog clamp was placed across the SMA for temporary occlusion. Note the intestinal pallor that was immediately evident upon occlusion. **aiii)** Following removal of the Bulldog clamp and reinstatement of blood flow, a hyperaemic flush was evident to the intestines. **b)** Representative graph showing current generated at the working electrode of the sensor during continuous sensor readings over a period of 70 min. Three cycles of 5 min occlusion followed by 10 min of reperfusion were performed in each animal before euthanasia. **c)** Combined analysis comparing current generated at the working electrode of the sensor during periods of SMA occlusion and intestinal reperfusion; results show mean current readings of the final 3 min of each occlusion period and final 5 min of each reperfusion period (one-way ANOVA with Holm-Šídák multiple comparisons test; data expressed as mean ± SEM, n=4, **p≤0.01).

	Baseline	Occlusion (1)	Reperfusion (1)	Occlusion (2)	Reperfusion (2)	Occlusion (3)	Reperfusion (3)	Euthanasia
Current (nA)	-1.98 ± 0.47	-0.12 ± 0.25	-1.73 ± 0.40	-0.41 ± 0.24	-1.85 ± 0.36	-0.28 ± 0.27	-1.84 ± 0.32	0.04 ± 0.16

Table I. Current readings generated during each superior mesenteric artery occlusion and reperfusion period and euthanasia (n=4; mean ± SEM).

Oxygen current generated by the sensor responded rapidly to alterations in inspired oxygen concentrations

To assess whether the sensor could detect changes in intestinal oxygenation through alterations in FiO_2 we performed sequential inspired O_2 challenges varying from 0.1-1.0 (n=5). With an FiO_2 of 0.21 (breathing room air), the mean sensor current was -1.35 ± 0.06 nA. When FiO_2 was reduced to 0.1, the sensor current decreased by more than half, to -0.60 ± 0.10 nA. This decrease was statistically significant when compared to currents generated when breathing room air (p= 0.0396). The decrease in current occurred over 1-2 min and was maintained throughout the hypoxaemic challenge. Following restoration of FiO_2 to 0.21, the current returned to baseline levels over a period of 1-2 min. Upon increasing inspired FiO_2 to 1.0 the sensor current rose to -6.53 ± 0.46 nA, which was statistically significant when compared to currents generated with an FiO_2 of 0.21 (p< 0.0001). This increase in current was again maintained throughout the FiO_2 challenge. Returning FiO_2 back to room air saw sensor currents return to baseline levels. Following euthanasia, sensor readings fell to the lowest recorded, measuring -0.08 ± 0.17 nA (Fig 6a). These results showed that the sensor could quickly, reliably and reproducibly detect changes in intestinal oxygenation following alterations in FiO_2 (Fig 6b and Table II).

Blood-gas analysis at the end of each FiO_2 challenge showed the expected physiological alterations in arterial O_2 partial pressure (PaO_2) and haemoglobin O_2 saturation (SaO_2). Both variables decreased significantly at an FiO_2 of 0.1, increased significantly at an FiO_2 of 1.0 (more prominent with PaO_2), and returned to baseline levels at 0.21. Total haemoglobin (Hb) concentration remained constant (Fig. 6c & d).

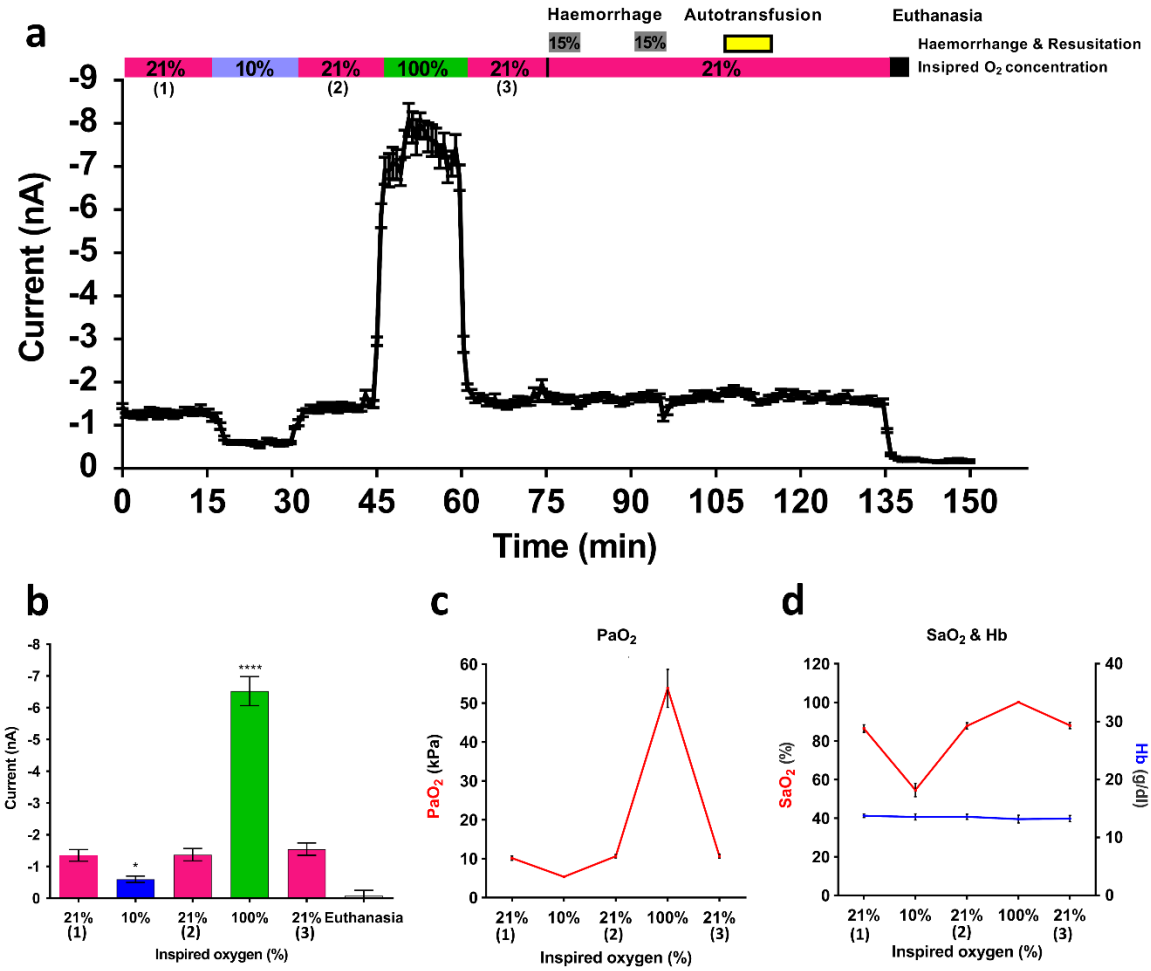

Figure 6. Sensor readings and physiological data obtained from assessing intestinal tissue oxygenation following changes in inspired O_2 concentrations (Protocol 3A). a) Representative graph showing current generated at the working electrode of the sensor during continuous sensor readings over a period of 150 min. 15 min blocks of each FiO_2 challenge were performed before beginning the removal of 30% of the circulating blood volume. **b)** Combined analysis comparing current generated at the working electrode of the sensor during each FiO_2 challenge; results show mean current readings of the final 5 min of each 15 min period (one-way ANOVA with Holm-Šídák multiple comparisons test; data expressed as mean ± SEM, n=5, ****$p \leq 0.0001$; *$p \leq 0.05$). **c&d)** Arterial O_2 partial pressure, total haemoglobin and haemoglobin O_2 saturation measured at end of each FiO_2 challenge.

	21% (1)	10%	21% (2)	100%	21% (3)	Euthanasia
Current (nA)	-1.35 ± 0.18	-0.60 ± 0.10	-1.37 ± 0.12	-6.53 ± 0.46	-1.55 ± 0.20	-0.08 ± 0.17

Table II. Current readings generated during each FiO_2 challenge and euthanasia (n=5; mean ± SEM).

No change in sensor current was identified following progressive haemorrhage

Following completion of FiO_2 challenges, we assessed the ability of the sensor to detect changes in intestinal ptO_2 following progressive withdrawal of 30% circulating blood volume

(performed in 2x 15% removal periods) (n=5) (Fig 7a). Physiological data obtained 10 min after the end of each haemorrhage procedure showed the expected physiological response occurring from acute haemorrhage: HR, MAP and Hb concentration all showed a moderate decrease after 15% removal, which was even more pronounced after 30%; HR decreased from 405 ± 22 bpm to 348 ± 16 bpm, MAP decreased from 118 ± 12 mmHg to 56 ± 3 mmHg, and Hb decreased from 13.3 ± 0.6 g/dl to 11.4 ± 0.4 g/dl. All of these physiological parameters returned to baseline levels following autotransfusion (Fig. 7b & c). SaO_2 remained constant throughout each haemorrhage procedure.

Despite these expected physiological responses to acute haemorrhage, only a small and non-significant decrease in sensor current was observed. Baseline measurements were -1.55 ± 0.20 nA; however, following 15% and 30% haemorrhage currents only decreased to -1.39 ± 0.13 nA and -1.33 ± 0.13 nA respectively. Following autotransfusion, no statistically significant changes in sensor current occurred, measuring -1.22 ± 0.14 nA at the end of the transfusion (Table III).

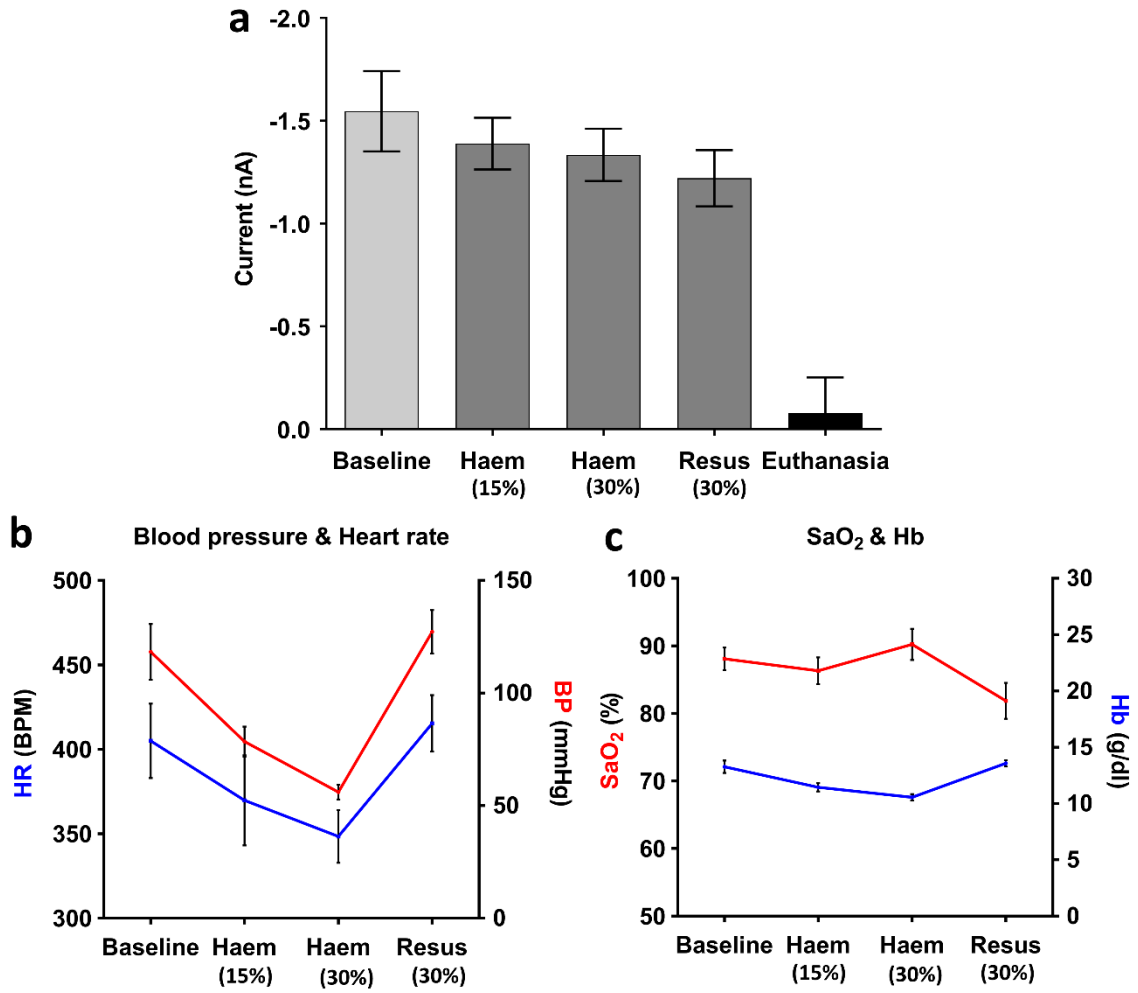

Figure 7. Sensor readings and physiological data obtained from assessing intestinal tissue oxygenation following progressive haemorrhage and autotransfusion (Protocol 3B). a) Combined analysis comparing current generated at the working electrode of the sensor during the preceding 15 min baseline period at 21% O_2 and the subsequent 2 cycles of removal of 15% circulating blood volume followed by autotransfusion; results show mean current readings of the final 5 min of each period (one-way ANOVA with Holm-Šídák's multiple comparisons test; data expressed as mean ± SEM, n=5). **b&c)** Mean arterial blood pressure, heart rate, total haemoglobin and haemoglobin O_2 saturation measured at end of each of intervention period (haem: haemorrhage; Resus: autotransfusion resuscitation).

	Baseline	15% haemorrhage	30% haemorrhage	Autotransfusion
Current (nA)	-1.55 ± 0.20	-1.39 ± 0.13	-1.33 ± 0.13	-1.22 ± 0.14

Table III. Current readings generated during 21% FiO_2, each haemorrhage procedure and autotransfusion (n=5; mean ± SEM).

Discussion

For validation and proof-of-concept that the IMPACT O_2 sensor can provide real-time measurements of intestinal ptO_2 we developed an *in vivo* intestinal ischaemic (SMA occlusion)

and hypoxic (changes in FiO_2) model. Control experiments were first used to demonstrate that the rats could remain physiologically stable under general anaesthesia and that the sensors provided stable measurements. These experiments also allowed us to rule out potential effects of the tissue environment on sensor stability; the design and packaging of the IMPACT O_2 sensor is likely to have minimised this potential problem. The outer protective coating is made from Nafion, an ionomer made by the addition of sulfonic acid groups to Teflon. Nafion membranes are commonly used in a variety of implantable devices due to the selectively of substances which diffuse through it. The pore size within the membrane is sufficiently small to exclude macromolecules such as proteins that may contaminate the electrode surface, while the presence of charged sulphonate groups leads to the electrostatic exclusion of small anions (34).

Our sensors were placed onto the intestinal serosal surface and secured with tissue glue. This technique avoided the use of constant manual pressure on the sensor which could interfere with intestinal blood supply leading to alterations in ptO_2 measurements (40). The tissue area from which the electrode measures ptO_2 is related to electrode size, a matter which needs to be considered if Clark electrodes are used for clinical applications. The working electrode (where O_2 is detected) of the IMPACT O_2 sensor has a diameter of 50 µm. This small sensing area means the sensor will not significantly deplete tissue O_2 levels, while also allowing for accurate sensor placement to specific areas by the surgeon. Use of multiple sensors would provide ptO_2 readings from a larger area, which is advantageous for anastomotic surgery as sensors could be placed around the anastomotic circumference and at either side of the resection site, giving detailed peri-anastomotic ptO_2 information. Such detailed information could not be achieved using a sensor with a large working area that gives only mean ptO_2

readings from multiple capillary beds, as is likely the case in the pre-clinical and clinical studies using Clark electrodes described in the introduction.

The SMA is the principal arterial supply to a large part of the gastrointestinal tract (from the lower part of the duodenum through to the proximal two-thirds of the transverse colon, and pancreas); its occlusion is the most direct way of causing intestinal ischaemia. Various SMA occlusion techniques have been documented in previous studies for the investigation of ischaemic intestinal insults, including ischaemia-reperfusion injuries (14, 22), cytokine production and bacteria/endotoxin translocation (16). In our study we performed temporary SMA ligation close to its aortic origin to ensure that no collateral circulation from any of its branches (inferior pancreaticoduodenal, intestinal, ileocolic, right and middle colic) could supply the region of small intestine of interest. Our results showed that within 1-2 min following SMA occlusion the current generated by the sensor fell to almost 0 nA, indicating a fully hypoxic state. This fall in current will be related to ischaemia and utilisation of the residual available O_2 by the tissues. Reperfusion of the intestine led to both visual changes in the tissue (hyperaemic flush and reoccurrence of mesenteric arterial pulsations) and a rapid raise in sensor current, indicating a return of normal oxygenation status to the intestine. This shows that the sensor reliably and reproducibly detects tissue hypoxia.

Following confirmation that changes in intestinal ptO_2 could be detected through ischaemic insults we determined if alterations in blood oxygenation, through changes in FiO_2, could be detected. Arterial blood-gas analysis confirmed the expected physiological responses to FiO_2 challenges. Hypoxaemia caused a decrease in PaO_2 and SaO_2, whereas hyperoxaemia led to an increase in their levels. Sensor current readings mirrored these results which changed in

accordance with FiO_2. Response times, as with ischaemia, were rapid, with the sensor giving stable currents 1-2 min after a FiO_2 change.

Although changes in intestinal ptO_2 were detected though SMA occlusion and FiO_2 alterations, no such changes were evident with acute haemorrhage. The reductions in HR and BP following 30% removal of circulating blood volume are consistent with increased vagal activity and reduced sympathetic input (Bezold–Jarish-like reflex), resulting in a decrease in total peripheral resistance. Only with more profound reductions in circulating blood volume is HR likely to increase during haemorrhage, representing a transition from reversible to irreversible shock (37). Although a slight decrease in Hb concentration was noted with 30% haemorrhage, SaO_2 levels remained consistent. Stable SaO_2 levels were likely due to the haemorrhage procedures being performed using an FiO_2 of 0.21. This level of SaO_2 in combination with a decrease in peripheral resistance may have been sufficient to maintain intestinal ptO_2, which could explain why no change in sensor currents were observed.

One of the main advantages of our experiments over previous published studies is that they were designed not only to assess whether our sensor could detect a change in intestinal ptO_2 following an initial physiological challenge, but also whether sensor readings could reverse to baseline levels upon removal of the challenge. Previous work has mainly reported results using individual measurements at specific time points (26, 39-41); the continuous recording of data performed in this study provided an opportunity to dynamically measure ptO_2 changes before, during and after each challenge. Our results reproducibly showed that sensor currents returned to baseline levels following each challenge.

For any implantable medical device to gain clinical approval it must undergo biocompatibility evaluation to assess biofunctionality (performance) and biosafety (local and systemic tissue

responses and the absence of carcinogenesis, mutagenesis and cytotoxicity) (4, 30, 36). Following implantation medical devices can lose functionality, largely due to biofouling (non-specific protein absorption) and the production of granulation and fibrous tissue around the implanted device (2). This process, known as the foreign body response (FBR), is composed of both acute and chronic inflammatory phases (2, 30, 31) and represents a clinical challenge in implantable technology design and development. The materials used in the manufacture of the IMPACT sensor have previously undergone extensive biocompatibility in both normal and diseased tissues, with results indicating that the materials are well tolerated with a minimal FBR elicited when implanted *in vivo*. These results have led to the use of these materials in a variety of medical devices (15). Although the FBR was not evaluated in this study, it is possible that acute inflammation could occur through either intestinal manipulation, placement of the sensor on the intestinal serosal surface or through the use of tissue glue to secure the sensor in place. In order to minimise these potential effects, the intestine was handled as little as possible and the glue was placed away from the sensors sensing area. Chronic inflammation was also not evaluated in this study largely due to the short-term nature of the experiments; however, we anticipate that in a clinical situation the effects from chronic inflammation may not be a significant issue. Fibrous reactions that occur around implantable devices occur mainly during the chronic inflammatory phase (5-21 days post implantation) (1); as the majority of anastomotic leaks occur within the first 8 days post-surgery (18) the use of a long-term implantable device is unlikely to be needed, this situation would reduce concerns regarding the impact that chronic inflammation can have on sensor functionality.

One potential limitation to these experiments is that both the SMA occlusion technique and alterations in FiO_2 (0.1 to 1.0) represent extreme experimental insults that may not accurately represent physiological ischaemic and hypoxaemic changes that occur following intestinal

surgery. However, the primary aim of this study was to validate the ability of the IMPACT sensor to measure dynamic changes in intestinal ptO_2; our results provide justification to progress validation experiments into more complex large animal anastomotic leak models. Pigs are regarded as excellent gastrointestinal translational models as they offer similarities in size, anatomy and physiology to that of humans and a porcine rectal anastomotic leak model has been described in the literature (43). Development of this porcine model could be performed for use in future experiments with the IMPACT O_2 sensor. These next phase experiments would investigate the sensors potential to monitor intestinal ptO_2 in normal physiological conditions and in those situations associated with an anastomotic leak and assess the suitability of the sensors for surgical implantation. Medium to long-term duration experiments would also allow the FBR and its effects on sensor functionality to be investigated. The use of this model would also allow evaluation of feasibility of placing multiple sensors, not only at the anastomotic site, but also at multiple sites along the gastrointestinal tract. These studies will elucidate the potential of the sensors to be used in human patients for the early detection of anastomotic leakage and the hypoperfusion that may precede it. Experiments will also provide clinical, haematological and biochemical indicators of anastomotic leakage and the development of septic peritonitis.

For the IMPACT O_2 sensors to be used clinically for resection and anastomotic applications investigations will need to be carried out to determine how these sensors could be placed intra-operatively, at the anastomotic site, or at multiple sites along the gastrointestinal tract so that they remain *in situ* and are able to measure post-operative intestinal ptO_2. Potential solutions would include their use akin to a surgical drain or through sensor incorporation into surgical staples. Drains are used commonly in anastomotic surgery (20, 33, 35) and are not associated with any significant complications. Placed in the region of the anastomotic site,

the drains exit the abdominal cavity through a skin incision which are then connected to external drainage bags and are easily removed when no longer required. Drains have been used to obtain post-operative peritoneal samples from anastomotic sites for measuring bacterial colonisation, cytokines (12) and metabolites (32) that might serve as indicators of early anastomotic leakage. We propose that designing the IMPACT O_2 sensor in a similar manner to a surgical drain would allow easy clinical use. The sensors, along with an electrical lead (similar in design to the current IMPACT O_2 sensor and lead wire), could be positioned on the intestine next to the anastomosis site at the time of surgery. The electrical lead would then pass out through the skin, like that of a surgical drain, allowing the sensor to be connected to the end-of-bed monitor, providing post-operative, real-time data on peri-anastomotic intestinal ptO_2 levels. The sensors could then be removed, in the same way as a surgical drain would be, when no longer required. The advantage of this approach would be that the IMPACT O_2 sensor would not require significant further development. Incorporation of IMPACT O_2 sensors into staples would have the advantage that peri-anastomotic ptO_2 could be measured around the entire circumference of the intestine, thus providing detailed spatial information. However, further technological development of the sensor through miniaturisation and the development of wireless technology would be required in order to achieve sensor integration into surgical staples. If these engineering advancements could be achieved it would provide opportunities for placing multiple sensors throughout the gastrointestinal tract, this concept could be utilised for measuring mucosal ptO_2 for other intestinal conditions where microenvironmental mucosal hypoxia can influence disease outcomes such as chronic intestinal inflammation (42).

Conclusion

Using our developed rodent model of small intestinal ischaemia and hypoxaemia, we successfully demonstrated that the IMPACT O_2 sensor can detect dynamic changes in intestinal oxygenation through ischaemic insults, alterations in FiO_2 and euthanasia. These miniaturised sensors have significant advantages over Clark O_2 sensors previously used in the literature as they have the potential be used during surgery and be left *in situ* following surgery to provide post-operative, minimally-invasive, continuous, real-time data regarding transitory changes in tissue ptO_2. This novel method of monitoring tissue perfusion could, for example, detect early peri-anastomotic tissue hypoxia and identify patients that may benefit from treatments to improve local oxygenation and prevent a leak. The sensors capability to detect dynamic intestinal oxygenation changes could also be used to assess treatment responses and, when combined with information gained from conventional monitoring systems, would help provide a more accurate assessment of the patient's condition. We expect that this type of visceral surface oximetry will prove clinically useful in the evaluation of bowel perfusion and may also be a powerful tool in many other clinical and research applications where measurement of organ perfusion is required, for example in transplant surgery, chronic intestinal ischaemia and inflammation, plastic surgery and brain injury.

Conflict of Interest Statement

The authors declare that they have no competing interests.

Authors' Contributions

DA, AM and MP secured funding for this research and conceptualised the initial work. MG and JRKM conceptualised the experiments, performed, analysed and interpreted the majority of the laboratory work with contributions from AD and MS. MG wrote the majority of the

manuscript with contributions from both JRKM and JM. Critical revisions were made from all authors. All authors read and approved the final manuscript.

References

1. **Anderson JM**. Biological responses to materials. *Annual Review of Materials Research* 31: 81-110, 2001.

2. **Anderson JM, Rodriguez A, and Chang DT**. Foreign body reaction to biomaterials. *Seminars in Immunology* 20: 86-100, 2008.

3. **Armstrong G, Croft J, Corrigan N, Brown JM, Goh V, Quirke P, Hulme C, Tolan D, Kirby A, Cahill R, O'Connell PR, Miskovic D, Coleman M, and Jayne D**. IntAct: intra-operative fluorescence angiography to prevent anastomotic leak in rectal cancer surgery: a randomized controlled trial. *Colorectal Disease* 20: 226-234, 2018.

4. **Arshady R**. *Polymeric biomaterials: chemistry, concepts, criteria. In: Introduction to polymeric biomaterials: the polymeric biomaterials series*. London: Citrus Books, 2003.

5. **Benaron DA, Parachikov IH, Friedland S, Soetikno R, Brock-Utne J, van der Starre PJA, Nezhat C, Terris MK, Maxim PG, Carson JJL, Razavi MK, Gladstone HB, Fincher EF, Hsu CP, Clark FL, Cheong W, Duckworth JL, and Stevenson DK**. Continuous, Noninvasive, and Localized Microvascular Tissue Oximetry Using Visible Light Spectroscopy. *Anesthesiology: The Journal of the American Society of Anesthesiologists* 100: 1469-1475, 2004.

6. **Boccola MA, Buettner PG, Rozen WM, Siu SK, Stevenson ARL, Stitz R, and Ho Y-H**. Risk Factors and Outcomes for Anastomotic Leakage in Colorectal Surgery: A Single-Institution Analysis of 1576 Patients. *World Journal of Surgery* 35: 186-195, 2011.

7. **Boyle N, Manifold D, Jordan M, and Mason R**. Intraoperative assessment of colonic perfusion using scanning laser doppler flowmetry during colonic resection1. *Journal of the American College of Surgeons* 191: 504-510, 2000.

8. **Daniel KD, Kim GY, Vassiliou CC, Galindo M, Guimaraes AR, Weissleder R, Charest A, Langer R, and Cima MJ**. Implantable diagnostic device for cancer monitoring. *Biosensors and Bioelectronics* 24: 3252-3257, 2009.

9. **den Dulk M, Noter SL, Hendriks ER, Brouwers MA, van der Vlies CH, Oostenbroek RJ, Menon AG, Steup W-H, and van de Velde CJ**. Improved diagnosis and treatment of anastomotic leakage after colorectal surgery. *European journal of surgical oncology* 35: 420-426, 2009.

10. **Dyson A, Stidwill R, Taylor V, and Singer M**. The impact of inspired oxygen concentration on tissue oxygenation during progressive haemorrhage. *Intensive Care Medicine* 35: 1783-1791, 2009.

11. **Dyson A, Stidwill R, Taylor V, and Singer M**. Tissue oxygen monitoring in rodent models of shock. *American journal of physiology Heart and circulatory physiology* 293: H526-533, 2007.

12. **Fouda E, El Nakeeb A, Magdy A, Hammad EA, Othman G, and Farid M**. Early detection of anastomotic leakage after elective low anterior resection. *Journal of Gastrointestinal Surgery* 15: 137-144, 2011.

13. **Friedland S, Benaron D, Coogan S, Sze DY, and Soetikno R**. Diagnosis of chronic mesenteric ischemia by visible light spectroscopy during endoscopy. *Gastrointestinal Endoscopy* 65: 294-300, 2007.

14. **Gordeeva AE, Temnov AA, Charnagalov AA, Sharapov MG, Fesenko EE, and Novoselov VI**. Protective Effect of Peroxiredoxin 6 in Ischemia/Reperfusion-Induced Damage of Small Intestine. *Digestive Diseases and Sciences* 60: 3610-3619, 2015.

15. **Gray ME, Meehan J, Blair EO, Ward C, Langdon SP, Morrison LR, Marland JR, Tsiamis A, Kunkler IH, and Murray A**. Biocompatibility of common implantable sensor materials in a tumor xenograft model. *Journal of Biomedical Materials Research Part B: Applied Biomaterials* 1-14, 2018.

16. **Grotz MR, Ding J, Guo W, Huang Q, and Deitch EA**. Comparison of plasma cytokine levels in rats subjected to superior mesenteric artery occlusion or hemorrhagic shock. *Shock (Augusta, Ga)* 3: 362-368, 1995.

17. **Hallböök O, and Sjödahl R**. Anastomotic leakage and functional outcome after anterior resection of the rectum. *British journal of surgery* 83: 60-62, 1996.

18. **Hyman N, Manchester TL, Osler T, Burns B, and Cataldo PA**. Anastomotic Leaks After Intestinal Anastomosis: It's Later Than You Think. *Annals of Surgery* 245: 254-258, 2007.

19. **Karliczek A, Benaron D, Baas P, Zeebregts C, Wiggers T, and Van Dam G**. Intraoperative assessment of microperfusion with visible light spectroscopy for prediction of anastomotic leakage in colorectal anastomoses. *Colorectal Disease* 12: 1018-1025, 2010.

20. **Karliczek A, Jesus E, Matos D, Castro A, Atallah A, and Wiggers T**. Drainage or nondrainage in elective colorectal anastomosis: a systematic review and meta-analysis. *Colorectal Disease* 8: 259-265, 2006.

21. **Kingham TP, and Pachter HL**. Colonic anastomotic leak: risk factors, diagnosis, and treatment. *Journal of the American College of Surgeons* 208: 269-278, 2009.

22. **Kozar RA, Holcomb JB, Hassoun HT, Macaitis J, DeSoignie R, and Moore FA**. Superior mesenteric artery occlusion models shock-induced gut ischemia-reperfusion. *Journal of Surgical Research* 116: 145-150, 2004.

23. **Kube R, Mroczkowski P, Granowski D, Benedix F, Sahm M, Schmidt U, Gastinger I, and Lippert H**. Anastomotic leakage after colon cancer surgery: A predictor of significant morbidity and hospital mortality, and diminished tumour-free survival. *European Journal of Surgical Oncology (EJSO)* 36: 120-124, 2010.

24. **Kudszus S, Roesel C, Schachtrupp A, and Höer JJ**. Intraoperative laser fluorescence angiography in colorectal surgery: a noninvasive analysis to reduce the rate of anastomotic leakage. *Langenbeck's archives of surgery* 395: 1025-1030, 2010.

25. **Lee ES, Bass A, Arko FR, Heikkinen M, Harris EJ, Zarins CK, van der Starre P, and Olcott C**. Intraoperative Colon Mucosal Oxygen Saturation During Aortic Surgery. *Journal of Surgical Research* 136: 19-24, 2006.

26. **Locke R, Hauser CJ, and Shoemaker WC**. The use of surface oximetry to assess bowel viability. *Archives of Surgery* 119: 1252-1256, 1984.

27. **Marland JRK, Blair EO, Flynn BW, González-Fernández E, Huang L, Kunkler IH, Smith S, Staderini M, Tsiamis A, Ward C, and Murray AF**. Implantable Microsystems for Personalised Anticancer Therapy. In: *CMOS Circuits for Biological Sensing and Processing*Springer International Publishing, 2018, p. 259-286.

28. **Marra F, Steffen T, Kalak N, Warschkow R, Tarantino I, Lange J, and Zünd M**. Anastomotic leakage as a risk factor for the long-term outcome after curative resection of colon cancer. *European Journal of Surgical Oncology* 35: 1060-1064, 2009.

29. **Masi BC, Tyler BM, Bow H, Wicks RT, Xue Y, Brem H, Langer R, and Cima MJ**. Intracranial MEMS based temozolomide delivery in a 9L rat gliosarcoma model. *Biomaterials* 33: 5768-5775, 2012.

30. **Morais J, Papadimitrakopoulos F, and Burgess D**. Biomaterials/Tissue Interactions: Possible Solutions to Overcome Foreign Body Response. *The American Association of Pharmaceutical Scientists* 12: 188-196, 2010.

31. **Onuki Y, Bhardwaj U, Papadimitrakopoulos F, and Burgess DJ**. A Review of the Biocompatibility of Implantable Devices: Current Challenges to Overcome Foreign Body Response. *Journal of Diabetes Science and Technology* 2: 1003-1015, 2008.

32. **Pedersen ME, Qvist N, Bisgaard C, Kelly U, Bernhard A, and Pedersen SM**. Peritoneal Microdialysis. Earlydiagnosis of Anastomotic Leakage after Low Anterior Resection for Rectosigmoid Cancer. *Scandinavian Journal of Surgery* 98: 148-154, 2009.

33. **Petrowsky H, Demartines N, Rousson V, and Clavien P-A**. Evidence-based value of prophylactic drainage in gastrointestinal surgery: a systematic review and meta-analyses. *Annals of surgery* 240: 1074-1085, 2004.

34. **Rocchitta G, Spanu A, Babudieri S, Latte G, Madeddu G, Galleri G, Nuvoli S, Bagella P, Demartis MI, and Fiore V**. Enzyme biosensors for biomedical applications: Strategies for safeguarding analytical performances in biological fluids. *Sensors* 16: 780-801, 2016.

35. **Rondelli F, Bugiantella W, Vedovati M, Balzarotti R, Avenia N, Mariani E, Agnelli G, and Becattini C**. To drain or not to drain extraperitoneal colorectal anastomosis? A systematic review and meta-analysis. *Colorectal Disease* 16: 35-42, 2014.

36. **Schoen FR, and Anderson JM**. *Host response to biomaterials and thier evaluation. In: Biomaterials science: an introduction to materials in medicine.* San Diego: Elsevier, 2004.

37. **Secher NH, and Van Lieshout JJ**. Heart rate during haemorrhage: time for reappraisal. *The Journal of Physiology* 588: 19-23, 2010.

38. **Servais EL, Rizk NP, Oliveira L, Rusch VW, Bikson M, and Adusumilli PS**. Real-time intraoperative detection of tissue hypoxia in gastrointestinal surgery by wireless pulse oximetry. *Surgical endoscopy* 25: 1383-1389, 2011.

39. **Shandall A, Lowndes R, and Young HL**. Colonic anastomotic healing and oxygen tension. *British Journal of Surgery* 72: 606-609, 1985.

40. **Sheridan WG, Lowndes RH, and Young HL**. Intraoperative tissue oximetry in the human gastrointestinal tract. *The American Journal of Surgery* 159: 314-319, 1990.

41. **Sheridan WG, Lowndes RH, and Young HL**. Tissue oxygen tension as a predictor of colonic anastomotic healing. *Diseases of the colon & rectum* 30: 867-871, 1987.

42. **Taylor CT, and Colgan SP**. Regulation of immunity and inflammation by hypoxia in immunological niches. *Nature Reviews Immunology* 17: 774-785, 2017.

43. **Wenger FA, Szucsik E, Hoinoiu BF, Ionac M, Walz MK, Schmid KW, and Reis H**. A new anastomotic leakage model in circular double stapled colorectal anastomosis after low anterior rectum resection in pigs. *Journal of Investigative Surgery* 26: 364-372, 2013.

Figure and Table Legends

Figure 1. Intra-operative photographs depicting placement of central venous (jugular) and arterial (carotid) lines. a) A 2 cm ventral cervical skin incision is made. **b&c)** Cervical dissection is performed for identification and mobilisation of the right jugular vein. **d)** One untied suture is placed distally around the jugular vein and a second is placed proximally and tied securely, leaving approximately 1 cm of vein between the 2 sutures. **e)** A venotomy is created just distal to the proximal suture; the cannula is inserted and advanced into the vein approximately 2-3 cm before tying the distal suture around the vein and cannula. **f)** Cervical dissection is performed for identification of the left carotid artery and its isolation from the vagus nerve. **g)** One untied suture is placed distally around the carotid artery and a second is placed proximally and tied securely leaving approximately 1.5 cm of artery between the 2 sutures. A small clamp is added just proximal to the distal suture before placing a third untied suture. **h)** An arteriotomy is created between the 2 sutures and the cannula is inserted and advanced up to the clamp. **i)** The third suture is tied loosely over the cannula and the clamp is removed. **j)** The cannula is advanced a further 2 cm before tying the distal suture around the artery and cannula. Both vessels were cannulated using 0.96 mm outside diameter PVC tubing (Scientific Commodities Inc., Lake Havasu City, AZ, USA) and secured in place with 5-0 silk (Ethicon, UK).

Figure 2. Outline of experimental protocols and interventions. Protocol 1: Control animals with no interventions. Protocol 2: Superior mesenteric artery occlusion. Protocol 3: Alterations in FiO_2, haemorrhage and autotransfusion (resuscitation). Instrumentation encompassed: anaesthesia induction, surgical preparation, placement of arterial and venous lines and celiotomy. The sensor was placed on the serosal surface of the small intestine approximately half way through the stabilisation period. Continuous sensor readings were commenced following the achievement of stable baseline physiological variables and continued for 15 min following confirmation of death post-euthanasia.

Figure 3. Sensor picture and intra-operative photographs depicting intestinal placement of the sensor. a) Macroscopic image of the IMPACT miniaturised O_2 sensor. **b)** Intra-operative sensor placement on the serosal surface of a section of small intestine.

Figure 4. Sensor readings and physiological data obtained from control animals (Protocol 1). a) Current generated at the working electrode of the sensor during continuous sensor readings over a period of 165 min; results show mean current readings from the final 5 min of each 15 min period (one-way ANOVA with Holm-Šídák multiple comparisons test; data expressed as mean ± SEM, n=3, p=0.7244). **b)** Physiological data obtained throughout the experimental period (Hb: haemoglobin; ABE: arterial base excess; SaO_2: haemoglobin O_2 saturation; PaO_2: arterial O_2 partial pressure; $PaCO_2$: arterial CO_2 partial pressure; CT: core temperature; RR: respiratory rate; HR: heart rate).

Figure 5. Intra-operative photographs and sensor readings during temporary superior mesenteric artery occlusion (Protocol 2). ai) Identification of the SMA originating from the left side of the aorta at the level of the right renal vein joining the caudal vena cava; the vessel is robust and can withstand the manipulation required for isolation from its surrounding tissue and associated vein. **aii)** A Bulldog clamp was placed across the SMA for temporary occlusion. Note the intestinal pallor that was immediately evident upon occlusion. **aiii)**

Following removal of the Bulldog clamp and reinstatement of blood flow, a hyperaemic flush was evident to the intestines. **b)** Representative graph showing current generated at the working electrode of the sensor during continuous sensor readings over a period of 70 min. Three cycles of 5 min occlusion followed by 10 min of reperfusion were performed in each animal before euthanasia. **c)** Combined analysis comparing current generated at the working electrode of the sensor during periods of SMA occlusion and intestinal reperfusion; results show mean current readings of the final 3 min of each occlusion period and final 5 min of each reperfusion period (one-way ANOVA with Holm-Šídák multiple comparisons test; data expressed as mean ± SEM, n=4, **p≤0.01).

Figure 6. Sensor readings and physiological data obtained from assessing intestinal tissue oxygenation following changes in inspired O_2 concentrations (Protocol 3A). a) Representative graph showing current generated at the working electrode of the sensor during continuous sensor readings over a period of 150 min. 15 min blocks of each FiO_2 challenge were performed before beginning the removal of 30% of the circulating blood volume. **b)** Combined analysis comparing current generated at the working electrode of the sensor during each FiO_2 challenge; results show mean current readings of the final 5 min of each 15 min period (one-way ANOVA with Holm-Šídák multiple comparisons test; data expressed as mean ± SEM, n=5, ****p≤0.0001; *p≤0.05). **c&d)** Arterial O_2 partial pressure, total haemoglobin and haemoglobin O_2 saturation measured at end of each FiO_2 challenge.

Figure 7. Sensor readings and physiological data obtained from assessing intestinal tissue oxygenation following progressive haemorrhage and autotransfusion (Protocol 3B). a) Combined analysis comparing current generated at the working electrode of the sensor during the preceding 15 min baseline period at 21% O_2 and the subsequent 2 cycles of removal of 15% circulating blood volume followed by autotransfusion; results show mean current readings of the final 5 min of each period (one-way ANOVA with Holm-Šídák's multiple comparisons test; data expressed as mean ± SEM, n=5). **b&c)** Mean arterial blood pressure, heart rate, total haemoglobin and haemoglobin O_2 saturation measured at end of each of intervention period (haem: haemorrhage; Resus: autotransfusion resuscitation).

Table I. Current readings generated during each superior mesenteric artery occlusion and reperfusion period and euthanasia (n=4; mean ± SEM).

Table II. Current readings generated during each FiO_2 challenge and euthanasia (n=5; mean ± SEM).

Table III. Current readings generated during 21% FiO_2, each haemorrhage procedure and autotransfusion (n=5; mean ± SEM).